

1990

# A Simple Model for a Zinc/Bromine Flow Cell and Associated Storage Tanks

G. D. Simpson

*Texas A & M University - College Station*

Ralph E. White

*University of South Carolina - Columbia, white@cec.sc.edu*

Follow this and additional works at: [https://scholarcommons.sc.edu/eche\\_facpub](https://scholarcommons.sc.edu/eche_facpub)



Part of the [Chemical Engineering Commons](#)

## Publication Info

*Journal of the Electrochemical Society*, 1990, pages 1843-1846.

© The Electrochemical Society, Inc. 1990. All rights reserved. Except as provided under U.S. copyright law, this work may not be reproduced, resold, distributed, or modified without the express permission of The Electrochemical Society (ECS). The archival version of this work was published in the *Journal of the Electrochemical Society*.

<http://www.electrochem.org/>

DOI: 10.1149/1.2086813

<http://dx.doi.org/10.1149/1.2086813>

# A Simple Model for a Zinc/Bromine Flow Cell and Associated Storage Tanks

G. D. Simpson\* and R. E. White\*\*

Department of Chemical Engineering, Texas A&M University, College Station, Texas 77843

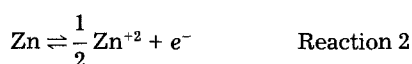
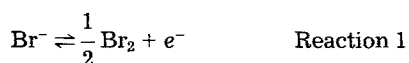
## ABSTRACT

A simple model for a parallel plate, zinc/bromine flow cell and associated storage tanks is presented and used to make time-dependent predictions for various quantities in the system. The model is based on a previously published algebraic model of the cell at steady-state and time-dependent, first-order differential equations for the storage tanks. The Butler-Volmer equation is used for the electrochemical reactions, and the homogeneous reaction between bromine and bromide is included. The model predictions indicate that the charging operation of a zinc/bromine battery can be significantly improved by using a storage tank with a larger residence time for the bromine side of the system.

Previous authors have modeled the zinc/bromine flow cell (1-6). Lee and Selman (1, 2) developed a model to determine the current density distribution along the electrode surfaces. Lee (3) extended that work to include time variations of the current density distribution in an attempt to predict dendrite formation. Van Zee *et al.* (4) developed a simplified model to describe overall cell performance. Mader and White (5) also developed a model that can be used to predict the overall cell performance by introducing a "one-step" approximation. Evans and White (6) extended that work by including a porous electrode and the capability of predicting round-trip energy efficiencies. They also presented a review of the modeling work that has been done on the zinc/bromine flow cell. More recently, Simpson and White (13) presented an algebraic model that is applicable to low-conversion reactors at steady state.

A zinc/bromine battery consists essentially of two electrodes, a porous separator and a pair of storage tanks. The separator is placed between the electrodes in such a way that there is a thin gap between each of the electrodes and the separator.

During charge, the principal reaction at the anode is the oxidation of  $\text{Br}^-$  to  $\text{Br}_2$ . At the cathode the principal reaction is the reduction of  $\text{Zn}^{+2}$  to  $\text{Zn}$ . An undesirable reaction at the cathode during charge is the reduction of  $\text{Br}_2$  to  $\text{Br}^-$ . A homogeneous phase bulk reaction occurs between  $\text{Br}_2$  and  $\text{Br}^-$  to yield  $\text{Br}_3^-$ . The two electrochemical reactions can be written in anodic form as



and the complexation reaction can be written as



The equilibrium constant for this homogeneous reaction is 17,000 ( $\text{cm}^3/\text{mol}$ ) (8).

The model presented herein is an extension of the work presented in Ref. (13). In the model development of Ref. (13), it is assumed that the concentration profiles within the reactor can be approximated by a series of constant and linear regions and that the potential profiles can be approximated by a series of linear regions as shown in Fig. 1. The regions of constant concentration correspond with perfectly mixed regions in the bulk of the electrolyte. The regions where the concentration profiles are linear are near the electrodes where both diffusion and migration are present. The potential profile is assumed to be linear through each region of the reactor. This work extends the work presented in Ref. (13) by including external storage

tanks and by making time-dependent predictions. The tanks are assumed to be perfectly mixed.

## Model Development

Simpson and White (13) presented an algebraic model for a parallel plate electrochemical reactor at steady state based on the schematic shown in Fig. 1. The major assumptions of that model are: (i) there is a diffusion region of known thickness in the electrolyte near each electrode; (ii) there is a perfectly mixed region a distance away from each electrode; and (iii) the electrolyte composition undergoes a step change from the inlet to the outlet composition within the reactor. This latter assumption is attributed to Mader and White (5) and is referred to by them as a "one-step" approximation. This "one-step" approximation is only applicable to low-conversion reactors. Other assumptions of the Simpson and White model are: (i) the system is isothermal; (ii) dilute solution theory applies; (iii) the flow is laminar in the reactor; and (iv) the Nernst-Einstein relationship (10) applies.

The work presented in Ref. (13) is extended here to include the external storage tanks by the inclusion of additional  $2n$  material balances. These equations are

$$\frac{dC_{\text{Br}_2}}{dt} = \frac{q_A}{V_{\text{TA}}} (\bar{C}_{\text{ai}} - C_{\text{Br}_2}) \quad [1]$$

for the tank on the anode side, and

$$\frac{dC_{\text{Zn}^{+2}}}{dt} = \frac{q_C}{V_{\text{TC}}} (\bar{C}_{\text{ci}} - C_{\text{Zn}^{+2}}) \quad [2]$$

for the tank on the cathode side. The inclusion of Eq. [1] and [2] allows the previous steady-state model of Simpson and White (13) to make time-dependent predictions for a complete reactor/tank system. Equations [1] and [2] may be dedimensionalized by using the following definitions

$$\tau = \frac{t q_C}{V_{\text{TC}}} \quad [3]$$

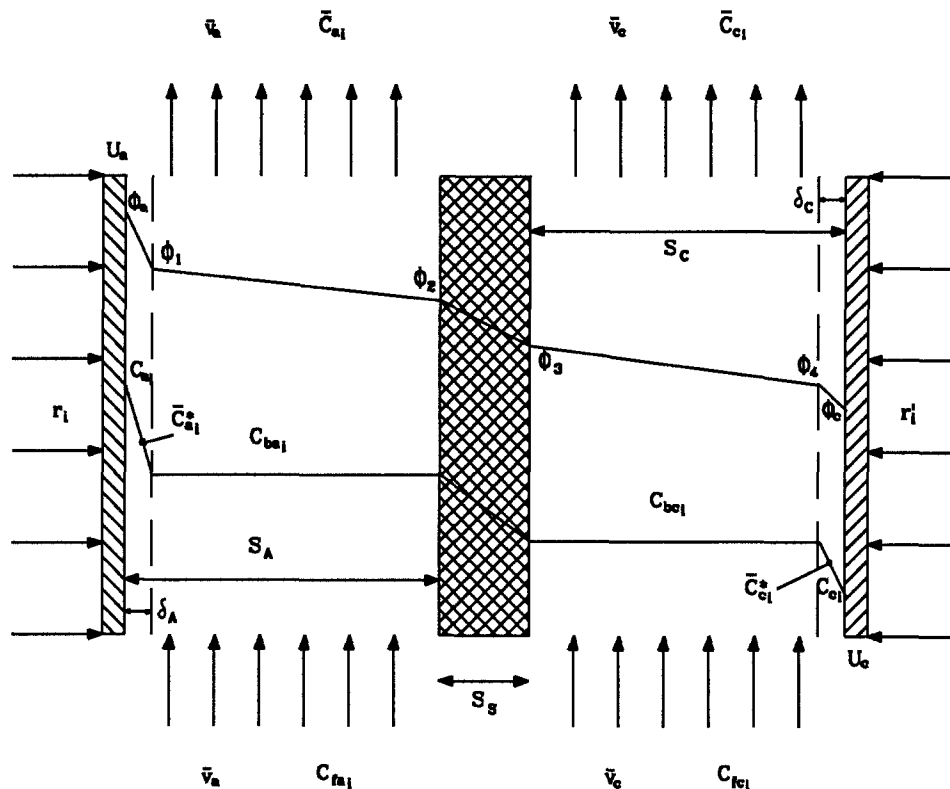
$$\mu = \frac{q_A V_{\text{TC}}}{q_C V_{\text{TA}}} \quad [4]$$

## Model Solution

Simpson (14) shows that the time dependence of a parallel plate flow cell with a feed recycle system can be approximated by a series of steady-state solutions if the residence time in the storage tanks is large. Each steady-state solution is obtained according to the method described in (13). The method shown there consists essentially of setting the left-hand sides of Eq. [10]-[14] of Ref. (13) equal to zero and solving the resulting set of algebraic equations. This approximation will hereafter be referred to as the pseudo steady-state approximation.

\* Electrochemical Society Student Member.  
\*\* Electrochemical Society Active Member.

Fig. 1. Schematic of Zn/Br<sub>2</sub> flow cell under charge conditions.



By assuming that the pseudo steady-state assumption is applicable, the operating conditions of the reactor can be determined for any set of feed compositions by using the steady-state calculation procedure of (13) and by solving the  $2n$  material balance equations for the storage tanks (*i.e.*, Eq. [1] and [2]) since these equations describe the time-dependence of each of the species concentrations in the respective feed streams. Values for the tank residence times ( $V_{TA}/q_A$  and  $V_{TC}/q_C$ ) must be specified prior to beginning the calculations. A fourth-order Runge-Kutta technique can be used to solve this system of ordinary differential equations. Thus, the solution algorithm used here consists of the following steps. First, given an initial set of feed compositions and values for the other input variables, the conditions within the reactor are determined by using the steady-state technique presented in (13). Note that it is assumed that this steady-state condition is reached instantly. Next, the Runge-Kutta technique is used to predict the feed compositions at the end of a time step by simultaneously integrating the  $2n$  material balance equations (Eq. [1] and [2]) that describe the time-dependence of the  $2n$  feed concentrations (*i.e.*,  $C_{Ai}$  and  $C_{Ci}$ ). Once the feed compositions at the end of the time step are determined, the method used in (13) (Newton-Raphson technique) is used to determine the new 'steady-state' operating conditions for the next time step. This process is repeated until the desired number of time steps have been taken.

### Discussion of Results

Figures 2-5 show the predicted response of the reactor and storage tanks during an extended period of charge at constant potential (see Ref. (13) for many of the input parameters for the model). Figure 2 shows that the current density decreases monotonically with time. This is due to the decrease in electrical conductivity that is associated with the removal of charged species from the electrolyte during charge.

Figure 3 shows that the coulombic efficiency at the cathode has a maximum value for each of the residence time ratios considered (for  $E_{cell} = 1.9V$ ). The coulombic efficiency has a maximum because of two conflicting tendencies. As the flow cell operates, the potential adjacent to the cathode increases. This increase in potential strongly favors the zinc reaction (due to the exchange current densities), and consequently the coulombic efficiency tends to increase. This tendency is offset by a tendency to decrease

that results from an increase in Br<sub>2</sub> concentration at the cathode surface. The increase in Br<sub>2</sub> concentration at the cathode surface is the result of an increase in Br<sub>2</sub> diffusion across the separator. This is ultimately the result of the increase in Br<sub>2</sub> concentration in the anodic feed during charge. Increasing the residence time ratio of the storage tanks retards the increase in Br<sub>2</sub> concentration in the anodic feed during charge. This results in an increase in the coulombic efficiency at the cathode.

Figure 4 shows the variation of the bromine concentration in the anodic feed during charge. The rate of bromine production is relatively constant throughout the charge

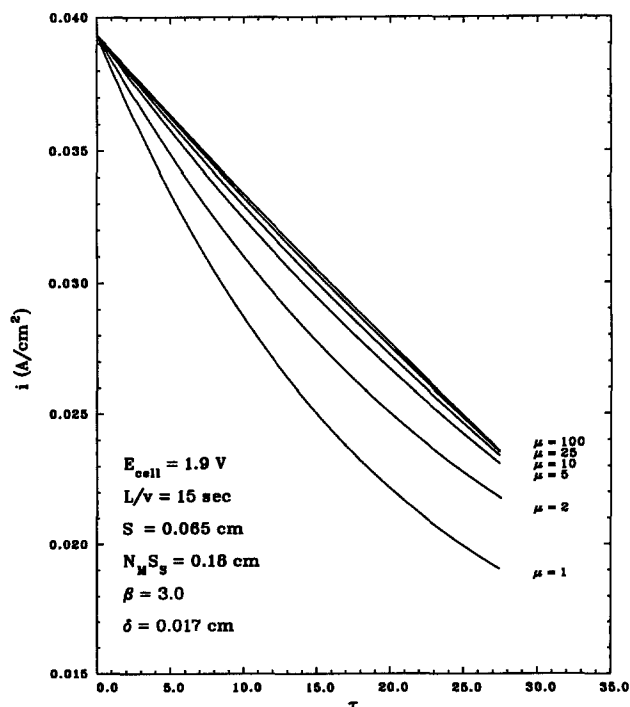


Fig. 2. Current density dependence on dimensionless time  $\tau$  as a function of residence time ratio  $\mu$ .

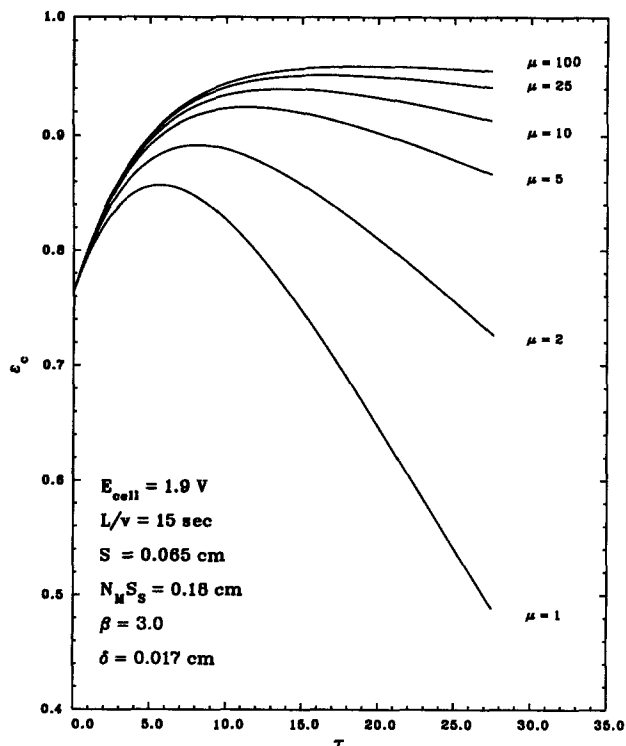


Fig. 3. Coulombic efficiency dependence on dimensionless time  $\tau$  as a function of residence time ratio  $\mu$ .

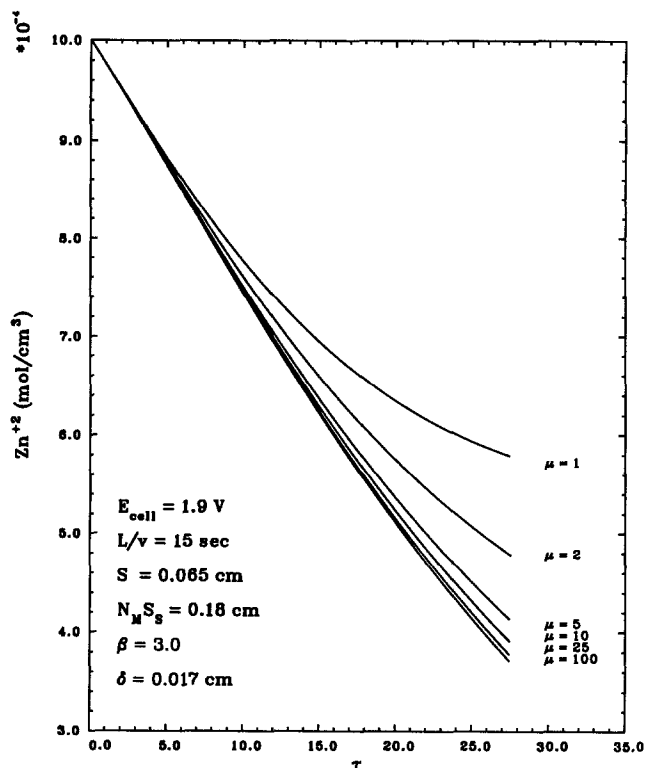


Fig. 5. Dependence of the  $Zn^{+2}$  concentration in the cathodic feed on dimensionless time  $\tau$  as a function of residence time ratio  $\mu$ .

cycle. Therefore, the slope of each of the curves is relatively constant.

Figure 5 shows the variation of the zinc ion concentration in the cathodic feed during charge. For a system with a tank residence time ratio equal to 1, the reaction rate for zinc approaches zero near the end of the charge cycle. This is ultimately due to the high concentration of bromine in the anodic feed. For efficient operation of a zinc/bromine battery, it is advisable to stop the charging process before the coulombic efficiency falls to such a low value. Other-

wise, most of the energy used by the cell in the latter portion of the charging cycle is wasted. For systems with a tank residence time ratio greater than 1, the reaction rate for zinc decreases more slowly. Therefore, the length of the useful charging cycle is increased.

### Conclusion

This work demonstrates that the time-dependent performance of a parallel plate flow cell with a feed recycle system can be approximated by a series of steady-state solutions when the residence times of the storage tanks are large compared to the residence time of the reactor. This work also demonstrates that the coulombic efficiency at the cathode during charge is significantly affected by the residence time in the bromine storage tank.

### Acknowledgment

The authors wish to acknowledge the support of this work by the National Science Foundation through Grant No. CBT-8620142.

Manuscript submitted June 21, 1989; revised manuscript received ca. Jan. 2, 1990.

Texas A & M University assisted in meeting the publication costs of this article.

### LIST OF SYMBOLS

- A projected area of porous electrode, cm<sup>2</sup>
- $A_{eff}$  effective area of porous electrode, cm<sup>2</sup>
- $C_{ai}$  concentration at the anode, mol/cm<sup>3</sup>
- $C_{bai}$  bulk region concentration on anode side, mol/cm<sup>3</sup>
- $C_{bci}$  bulk region concentration on cathode side, mol/cm<sup>3</sup>
- $C_{ci}$  concentration at the cathode, mol/cm<sup>3</sup>
- $C_{fa_i}$  feed concentration on anode side, mol/cm<sup>3</sup>
- $C_{fc_i}$  feed concentration on cathode side, mol/cm<sup>3</sup>
- $\bar{C}_{ai}$  average outlet concentration on anode side, mol/cm<sup>3</sup>
- $\bar{C}_{ci}$  average outlet concentration on cathode side, mol/cm<sup>3</sup>
- $\bar{C}_s$  average concentration in separator, mol/cm<sup>3</sup>
- $\bar{C}_{ea_i}$  average concentration near electrode on anode side, mol/cm<sup>3</sup>
- $\bar{C}_{ec_i}$  average concentration near electrode on cathode side, mol/cm<sup>3</sup>

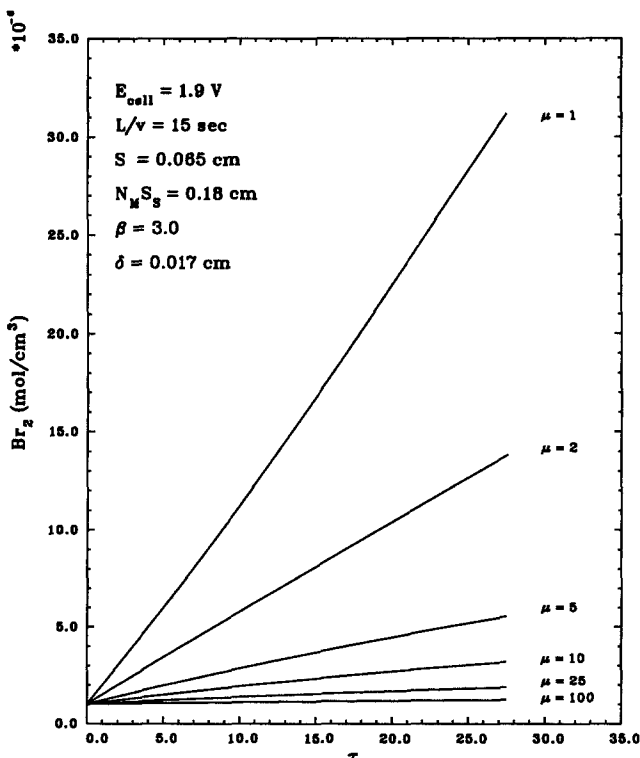


Fig. 4. Dependence of the concentration of bromine in the anodic feed on dimensionless time  $\tau$  as a function of residence time ratio  $\mu$ .

$\bar{C}_{a_i}^*$	velocity-averaged concentration near the anode, mol/cm <sup>3</sup>	$\phi_4$	electrolyte potential at interface between diffusion region and perfectly mixed region on cathode side, V
$\bar{C}_{c_i}^*$	velocity-averaged concentration near the cathode, mol/cm <sup>3</sup>	$\Delta\phi$	voltage drop through electrolyte and separator, V
$E_{\text{cell}}$	operating potential of reactor, V	$\epsilon_C$	current efficiency (6)
$i$	total current density, A/cm <sup>2</sup>	$\epsilon_T$	total efficiency (6)
$L$	reactor length, cm		
$n$	number of components		
$N_M$	Macmullin number		
$q_A$	volumetric flow rate through anode side, cm <sup>3</sup> /s		
$q_C$	volumetric flow rate through cathode side, cm <sup>3</sup> /s		
$S_A$	distance from anode surface to separator, cm		
$S_C$	distance from cathode surface to separator, cm		
$S_S$	distance across separator, cm		
$t$	time, s		
$T$	reactor temperature, K		
$U_a$	potential at anode, V		
$U_c$	potential at cathode, V		
$V_{TA}$	volume of storage tank on anode side, cm <sup>3</sup>		
$V_{TC}$	volume of storage tank on cathode side, cm <sup>3</sup>		
$\bar{v}_a$	average velocity through anode side, cm/s		
$\bar{v}_c$	average velocity through cathode side, cm/s		
$\beta$	area ratio for porous electrode, $A_{\text{eff}}/A$		
$\delta_A$	diffusion layer thickness near anode, cm		
$\delta_C$	diffusion layer thickness near cathode, cm		
$\mu$	ratio of residence times, cathodic side/anodic side (see Eq. [4])		
$\tau$	dimensionless time (see Eq. [3])		
$\phi_a$	electrolyte potential at anode surface, V		
$\phi_c$	electrolyte potential at cathode surface, V		
$\phi_1$	electrolyte potential at interface between diffusion region and perfectly mixed region on anode side, V		
$\phi_2$	electrolyte potential at separator on anode side, V		
$\phi_3$	electrolyte potential at separator on cathode side, V		

## REFERENCES

1. J. Lee and J. R. Selman, *This Journal*, **129**, 1670 (1982).
2. J. Lee and J. R. Selman, *ibid.*, **130**, 1237 (1983).
3. J. Lee, Ph. D. Dissertation, Illinois Institute of Technology, Chicago, IL (1981).
4. J. W. Van Zee, R. E. White, P. Grimes, and R. Bellows, in "Electrochemical Cell Design," R. E. White, Editor, p. 293, Plenum Publishing Co., New York (1984).
5. M. J. Mader and R. E. White, *This Journal*, **133**, 1297 (1986).
6. T. I. Evans and R. E. White, *ibid.*, **134**, 866 (1987).
7. T. I. Evans and R. E. White, *ibid.*, **134**, 2725 (1987).
8. M. Eigen and K. Kustin, *J. Am. Chem. Soc.*, **84**, 1355 (1962).
9. D. J. Pickett, "Electrochemical Reactor Design," Chap. 4-6, Elsevier Scientific Publishing Co., New York (1979).
10. J. S. Newman, "Electrochemical Systems," Chap. 11, Prentice-Hall Inc., Englewood Cliffs, NJ (1973).
11. V. Edwards and J. S. Newman, *This Journal*, **134**, 1181 (1987).
12. T. V. Nguyen, C. W. Walton, and R. E. White, *ibid.*, **133**, 1130 (1986).
13. G. D. Simpson and R. E. White, *ibid.*, **136**, 2137 (1989).
14. G. D. Simpson, M. S. Thesis, Texas A & M University, College Station, TX (1988).

# Technical Notes



## Three-Dimensional Current Distributions in a Bipolar, Chlor-Alkali Membrane Cell

R. E. White\* and F. Jagush\*\*

Department of Chemical Engineering, Texas A&M University, College Station, Texas 77843-3122

H. S. Burney\*

Dow Chemical U.S.A., Texas Applied Science Laboratories, Freeport, Texas 77541

The current distributions in a stack of bipolar, membrane chlor-alkali cells are important design considerations (1). The degree of nonuniformity of the current distribution is important to know because highly nonuniform current distributions could cause, among other things, severe damage to the membrane in a cell stack (2).

Recently, Dimpault-Darcy and White (3) used a computer program named TOPAZ2D (4), which is based on the finite element technique, to predict the two-dimensional current and potential distributions in a bipolar plate electrolyzer. In that paper they stated that TOPAZ3D (5) could be used to predict current and potential distributions for three spatial coordinates, but they did not present any results.

The finite element method has also been used by others (6-12) to predict current and potential distributions. However, most of these investigators used two spatial coordinates in their work. They used a two-dimensional method

to predict current and potential distributions in chlorine cells (6, 7), electroplating cells (8-10), and corrosion processes (11, 12). Morris and Smyrl (12) did use three spatial coordinates in some of their work, but they did not consider the spatial dependence of the specific conductivities, as done here. The purpose of this paper is to present the current distributions obtained by using TOPAZ3D for a three-dimensional section of bipolar, membrane chlor-alkali cell which includes portions that have spatial-dependent specific conductivities.

Figure 1 is a schematic of the section of a bipolar membrane cell (see Ref. (1) and (13) for a description of the cell) considered here. As shown in Fig. 1, a set current enters the anode from the boss portion of an anode/cathode element of the stack, passes through the various regions of the cell, and leaves through the boss portion of the next anode/cathode element. Only one quarter of a boss and the associated cell components are considered because of the symmetry of the components in the middle of the cell. Even though the results presented below do not apply to sections of the cell near the edge of the stack, the tech-

\* Electrochemical Society Active Member.

\*\* Electrochemical Society Student Member.